# Optimizing the Physicochemical Properties of Raf/MEK Inhibitors by Nitrogen Scanning

Toshihiro Aoki,[†] Ikumi Hyohdoh,[†] Noriyuki Furuichi,[†] Sawako Ozawa,[†] Fumio Watanabe,[†] Masayuki Matsushita,[†] Masahiro Sakaitani,[†] Kenji Morikami,[‡] Kenji Takanashi,[†] Naoki Harada,[†] Yasushi Tomii,[†] Koji Shiraki,[‡] Kentaro Furumoto,[‡] Mitsuyasu Tabo,[‡] Kiyoshi Yoshinari,[†] Kazutomo Ori,[†] Yuko Aoki,[†] Nobuo Shimma,[†] and Hitoshi Iikura*[,†,‡]

[†]Research Division, Chugai Pharmaceutical Co., Ltd., 200 Kajiwara, Kamakura, Kanagawa 247-8530, Japan
[‡]Research Division, Chugai Pharmaceutical Co., Ltd., 1-135 Komakado, Gotemba, Shizuoka 412-8513, Japan

S *Supporting Information*
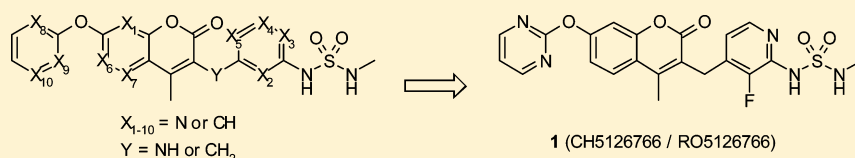
ABSTRACT: Substituting a carbon atom with a nitrogen atom (nitrogen substitution) on an aromatic ring in our leads **11a** and **13g** by applying nitrogen scanning afforded a set of compounds that improved not only the solubility but also the metabolic stability. The impact after nitrogen substitution on interactions between a derivative and its on- and off-target proteins (Raf/MEK, CYPs, and hERG channel) was also detected, most of them contributing to weaker interactions. After identifying the positions that kept inhibitory activity on HCT116 cell growth and Raf/MEK, compound **1** (CH5126766/RO5126766) was selected as a clinical compound. A phase I clinical trial is ongoing for solid cancers.

KEYWORDS: *Nitrogen scan, Raf, MEK, kinase inhibitor, CH5126766, RO5126766*

In the hit-to-lead process in medicinal chemistry, critical aspects in a compound are compatibility between the physicochemical properties, safety profiles, and bioactivity. However, a derivatization favorable for one factor (bioactivity, physicochemical properties, toxicity, etc.) often means that another factor fails the criteria set for its advancement to the clinic. To solve this paradox, one could attempt to improve one factor by using a chemical modification that minimally changes the conformation of a lead because the impact on other factors might be minimized. A fluorine atom substitution of a hydrogen atom attached to a carbon atom (fluorine substitution) is a representative example of such derivatization: when subsets of neighboring functional groups to the introduced fluorine are absent, changes in 3D conformation would be minimal compared to other modifications, and those of electronic properties would also be limited.[1−5]

Another approach is nitrogen substitution of aromatic moieties.[6−8] In nitrogen substitution, just as in fluorine substitution, 3D conformational changes of a lead compound could be smaller than other possible chemical modifications, if no critical functional groups that cause electronic repulsions or interactions are located in proximity to the introduced nitrogen. In contrast to fluorine substitution, nitrogen substitution derives inherently dramatic changes in the electronic properties.

Reflecting its ability to make such changes in electronic properties, nitrogen substitution has been utilized to modify various physicochemical properties and safety profiles. Improved water solubility has been reported,[9] with benefits to the resulting PK profile.[7] Decreasing hERG inhibitory activity of lipophilic leads[10−12] was found using nitrogen substitution of a benzene moiety.[13,14] Because CH−π interaction between a drug and the hERG channel are reported to be key regardless of the CLogP values,[15] nitrogen substitution of a phenyl ring could also be effective from this point of view. Effects on CYP interactions by nitrogen substitutions are still being elucidated: pyridine moiety has the potential to inhibit CYP by the interaction of the nitrogen to Fe,[16,17] while a report showed a compound after nitrogen substitution had reduced CYP inhibition compared to the parent.[6] Metabolic stability was improved in derivatives by nitrogen substitution of aromatic moieties,[8] which made them less susceptible to oxidative metabolism and also less lipophilic.

We recently reported SAR studies of a Raf and MEK inhibitor[2,18] that inhibits one of the most important signal transduction pathways in human cancer, the Ras/Raf/MEK/ERK pathway.[19] Introducing a sulfamide moiety to our coumarin hit afforded the compatibility of Raf/MEK activity and oral bioavailability.[18] Fluorine scanning allowed us to identify better leads;[2] because all the derivatives retained the physicochemical properties, we focused on identifying the positions for enhancing Raf/MEK activity (Scheme 1). Here we

Scheme 1. Fluorine Scanning and Nitrogen Scanning Led to Clinical Compound 1
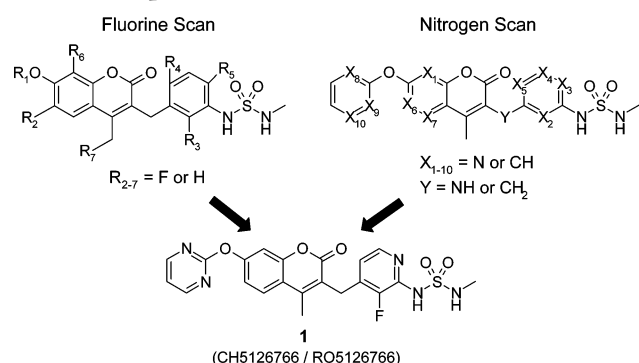

report another strategy, a nitrogen scan, in which conformational change of a lead would be smaller than other possible chemical modifications (C–H → C–NH$_2$, CH → C–OH, etc.). Nitrogen-substituted compounds of our leads **11a** and **13g**, which had room for improved solubility and metabolic stability, afforded positive effects on them, regardless of the nitrogen substitution positions (Scheme 1). This allowed us to focus on finding the positions that kept bioactivity, and we identified the clinical compound **1** (CH5126766/RO5126766), which showed superior antitumor effects compared to a pure MEK inhibitor in a mouse xenograft.[20]

A set of coumarin derivatives possessing nitrogens (compounds **1**, **11–13**, and **15**) was synthesized as shown in
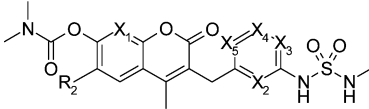
Scheme 2. Coumarin with nitrogen substituted at X$_2$–X$_5$ or Y was synthesized effectively in a manner similar to that reported previously.[21] Compounds **4c–f**, which were obtained by the alkylation of ethyl acetoacetate with bromomethylpyridines **3c–f**, were converted to coumarins **6c–f** via a typical Pechmann reaction with resorcinol **5a** or **5f**. After introducing the R$_1$ moiety, reaction with N-methylsulfamoyl chloride or N-methyl-2-oxooxazolidine-3-sulfonamide afforded the targets **11b–e** or **12f**. The fluorinated compound **4g** (X$_2$ = CF), which was obtained by the alkylation of ethyl acetoacetate with compound **3g**, was converted to target **1** or **13h–i**, as above. A coumarin substituted to nitrogen at the Y position was also obtained via Pechmann reaction of resorcinol (**5a**) and compound **4j**, which was prepared from the reaction of 3-nitroaniline (**3j**) with compound **9**[22] and subsequent hydrolysis. Converting to the target **11j** was smoothly achieved by reducing the nitro group and by subsequent sulfamoylation. In the case of the phenyl group at R$_1$, coumarin was formed by the reaction of compound **5g** instead of resorcinol (**5a**). Using Zn(OTf)$_2$ in MeOH for the Pechmann reaction instead of H$_2$SO$_4$ was crucial for obtaining coumarin **6b**, which has nitrogen at X$_1$.[23] Synthesis of 5- (X$_6$ = N) or 6-azacoumarin (X$_7$ = N) derivative was unsuccessful. An attempted Pechmann reaction using a typical condition (H$_2$SO$_4$) or modified conditions[24] (NH$_2$SO$_3$H, ZrCl$_4$, ZnCl$_2$, Sm(NO$_3$)$_3$, and AlCl$_3$) did not give the desired coumarin.

In the five compounds in Table 1 with nitrogen substituted at different positions, only one position (X$_3$) maintained inhibitory activity on HCT116 cell growth and Raf/MEK

Scheme 2. Synthesis of Coumarins 1, 11–13, and 15[a]
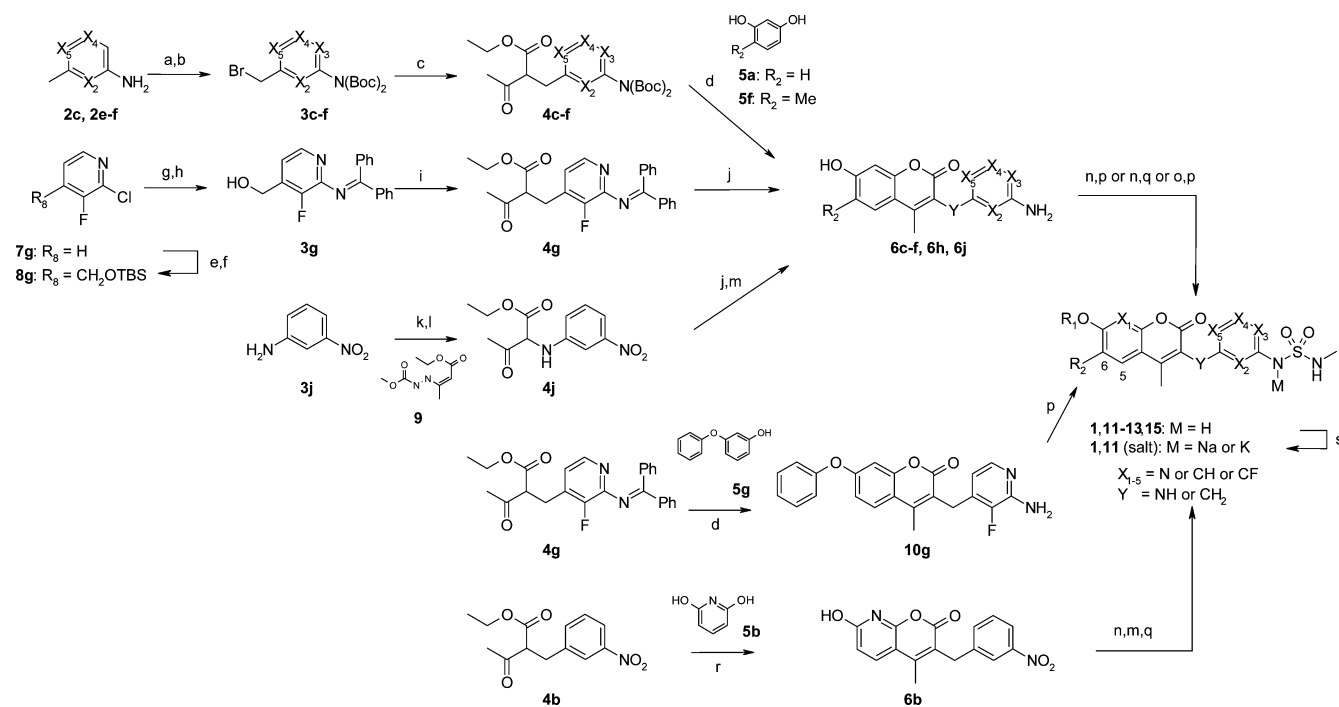
[a]Reagents and conditions: (a) (Boc)$_2$O, 60 °C, then (Boc)$_2$O, THF, DMAP, rt; (b) NBS, benzoylperoxide or AIBN, CCl$_4$, reflux; (c) ethyl acetoacetate, NaH, THF, 0 °C; (d) **5**, conc. H$_2$SO$_4$; (e) LDA, THF, DMF, –78 to 0 °C, then NaBH$_4$, 0 °C, 58%; (f) TBSCl, imidazole, THF, rt, 93%; (g) benzophenone imine, NaO^{t}Bu, Pd$_2$(dba)$_3$, rac-BINAP, toluene, 60 °C; (h) TBAF, THF, 76% (2 steps); (i) MsCl, LiO^{t}Bu, THF, 0 °C, then ethyl acetoacetate, LiO^{t}Bu, NaI, THF, 50 °C, 3 h, 95%; (j) **5a**, MsOH, CF$_3$CH$_2$OH; (k) **9**, THF, 70 °C, 12 h, 78%; (l) TiCl$_3$, 20–30% HCl aq., acetone, rt, 30 min, 71%; (m) SnCl$_2$·2H$_2$O, EtOAc, 75 °C; (n) R$_1$X, Cs$_2$CO$_3$ or K$_2$CO$_3$ or NaH, DMF; (o) R$_1$X, CuI, N,N′-dimethylethylenediamine, Cs$_2$CO$_3$, DMF, 100 °C; (p) N-methylsulfamoyl chloride, pyridine, DMF; (q) N-methyl-2-oxooxazolidine-3-sulfonamide, Et$_3$N, MeCN, 80 °C; (r) **5b**, Zn(OTf)$_2$, MeOH, reflux; (s) NaOH or KOH, MeOH.
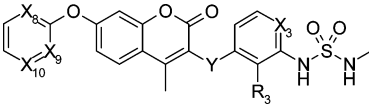
Table 1. Enzymatic and Cellular Activity and Pharmaceutical Properties of Coumarin Derivatives

| compd | R_2 | X_1 | X_2 | X_3 | X_4 | X_5 | IC$_{50}$ (nM) | | | | solubility (μg/mL) | CL$_{int}$ human (μL/min/mg) | PAMPA (10^{-6} cm/s) | AUC$_{po}$[a] (μM·h) |
							HCT116	HT-29	C-Raf	MEK1				
11a	H	CH	CH	CH	CH	CH	24	9	300	110	32	20	6	78[b]
11b	H	N	CH	CH	CH	CH	1100	600	2500	440	43	3	3	ND
11c	H	CH	N	CH	CH	CH	270	73	70	110	320	7	6	314
11d	H	CH	CH	N	CH	CH	32	25	32	99	55	6	7	134
11e	H	CH	CH	CH	N	CH	>10000	>10000	>50000	>50000	240	ND	ND	ND
12a	Me	CH	CH	CH	CH	CH	22	8	78	29	11	17	4	18
12f	Me	CH	CH	CH	CH	N	>10000	5700	27000	37000	425	ND	ND	ND

[a]Compounds were evaluated in 24 h exposure studies in mice at 100 mg/kg and formulated as solutions of 5% DMSO, 5% Cremophor EL, 15% PEG400, 15% HPCD, and 60% water. [b]Sodium salt was used.

Table 2. Enzymatic and Cellular Activity of Coumarin Derivatives

| compd | X_3 | X_8 | X_9 | X_{10} | Y | R_3 | IC$_{50}$ (nM) | | |
							HCT116	C-Raf	MEK1
13g	N	CH	CH	CH	CH$_2$	F	110	21	76
13h	N	N	CH	CH	CH$_2$	F	45	81	190
13i	N	N	CH	N	CH$_2$	F	900	56	650
1	N	N	N	CH	CH$_2$	F	40	56	160
14	CH	N	N	CH	CH$_2$	F	17	23	97
15j	CH	N	N	CH	NH	H	>10000	>50000	>50000

(compound **11d**), and none of the positions enhanced it. Introducing nitrogen at X_2 position resulted in decreased cell growth inhibitory activity by a factor of 10 (compound **11c**) compared with the parent **11a**. Compounds with a nitrogen substitution at X_1, X_4, and X_5 showed larger than 50-fold decreases in cell growth inhibitory activity.

On the other hand, all the evaluated compounds had improved water solubility and metabolic stability compared with the parent **11a** or **12a** (Table 1). Solubility was evaluated by the LYSA method (high-throughput solubility assay),[25] and the values of the compounds **11b** and **11d** were slightly more than that of **11a**, and those of **11c**, **11e**, and **12f** increased up to 40-fold. Metabolic stability was evaluated using human liver microsome, and all evaluated compounds were more stable (by more than 3-fold) than the parent **11a**. Because one of the metabolic positions of compound **11a** was previously identified as the phenyl ring bearing a sulfamide moiety,[18] decreasing the electron density of carbon atoms by replacing the aryl ring with a pyridyl ring (**11c** and **11d**) would be a reason for oxidative metabolism to persist. Membrane permeability evaluated by the PAMPA method[26] had high enough and comparable values to parent **11a**. After oral administration of compound **11c** or **11d** to mice, AUCs increased up to 4-fold, which could reflect the improved metabolic stability and/or solubility.

We also modified the X_{8-10} (R_1 part of Scheme 2) and Y part because modifying the carbamate part (R_1 part), which is a major metabolic site, seemed fruitful (Table 2).[18] Although the carbamate moiety was key for the strong bioactivity in our preliminary SAR,[18] we obtained compound **13g** (R_1 = Ph) with

acceptable cell inhibitory activity (IC$_{50}$ = 110 nM in HCT116 cell line) after random modification of the R_1 part by fixing R_3 to fluorine[2] and X_3 to nitrogen. Because the solubility as evaluated by the LYSA method was lower (18 μg/mL), nitrogen scanning at the R_1 position was performed. Compared to the parent compound **13g**, compound **13h** with nitrogen at X_8 position maintained the inhibitory activity on HCT116 cell growth and Raf/MEK. Although introducing an additional nitrogen at X_{10} position caused weaker inhibitory activity on cell growth (compound **13i**), introducing one at X_9 position (compound **1**[20]) afforded similar bioactivity to the parent **13g**. Introducing nitrogen at the Y position derived almost no bioactivity (compound **15j**). Nitrogen substitution improved solubility, and a high-throughput solubility assay of compounds **13g** and **1** showed 18 and 159 μg/mL, respectively. The AUC of compound **1** after oral administration to mice increased 36-fold (2831 μM·h) compared to the original **11a**. As just described, we succeeded in replacing a carbamate with a pyrimidyl moiety that was more metabolically stable. The effect of nitrogen substitution was also observed when the properties of compound **1** were compared to compound **14**,[2] which has C–H group at X_3 and nitrogen at X_8 and X_9. Metabolic stability (**1**, 0.5 μL/min/mg; **14**, 6.7 μL/min/mg), solubility (**1**, 159 μg/mL; **14**, 13 μg/mL), and AUC (**1**, 2831 μM·h; **14**, 425 μM· h) of compound **1** were all superior to those of compound **14** by around a factor of 10. As a result, by nitrogen scans at four additional positions (X_8, X_9, X_{10}, and Y), we identified the promising compound **1**, which has an IC$_{50}$ value of 40 nM on

HCT116 cell growth inhibitory activity and excellent solubility and AUC in mouse.

CYP or hERG inhibitory activity in the nitrogen-introduced derivatives was superior to that of the corresponding parents (Table 3). Nitrogen-introduced derivative **11d** showed almost

Table 3. CYP and hERG Inhibition of Coumarin

	CYP inhibition IC$_{50}$ (μM)[a]		
compd	2C9 (−/+)	3A4 (−/+)	hERG inhibiton[b] (%)
11a	29/96	13/5.6	ND
11d	>100/>100	>100/>100	ND
14	19/19	26/11	25
1	12/60	>100/>100	no inhibition

[a]IC$_{50}$ (−) and IC$_{50}$ (+) values were determined after a 30 min preincubation without and with NADPH, respectively. [b]At 10 μM.

no inhibition on CYP 2C9 and 3A4, while the parent **11a** showed CYP 3A4 inhibition at an IC$_{50}$ of 13 μM. This tendency is similar to a previous report,[6] while pyridine moiety itself has the potential to inhibit CYP. One possible explanation is that reducing lipophilicity of the molecule and/or decreasing electron density of carbon atoms on an aromatic ring by nitrogen substitution might be key to reducing the interaction to CYPs, which inherently have the function of modifying lipophilic compounds to hydrophilic compounds.[27−29] The same tendency was observed when comparing compounds **1** and **14**.

Our nitrogen scan at nine different positions resulted in us identifying three positions that kept bioactivity (Raf/MEK), six positions that decreased bioactivity at least 8-fold (Tables 1 and 2), and none that enhanced bioactivity. Because of the change in electronic structure to a more hydrophilic compound, derivatives after nitrogen substitution improved metabolic stability as well as solubility. The key to obtaining candidates with improved physicochemical properties is to identify the positions for nitrogen substitution at which the bioactivity will be acceptable. Decreased bioactivity could be explained by two possible reasons: reason 1 is that change of the whole 3D conformation after nitrogen substitution is critical and the compound could not achieve an active conformation; reason 2 is that change of the whole 3D conformation is minimal but electrostatic repulsion between the introduced nitrogen atom and target proteins is critical.

The effect on dihedral angles (ϕ1−ϕ6) was estimated by collecting crystal structures in the CSD data or by evaluation of potential energy surfaces at the B3LYP/6-31G(d) level (Figure 1A). Crystal data processing a diaryl ether part in CSD showed that stable conformations after nitrogen substitution at X$_8$ (blue), X$_9$ (green), and X$_{10}$ (red) overlapped well with those of the parent (black), and they had strong preferences for twisted structures (ϕ1 on 0°, 180°, and 360° and ϕ2 on 90° and 270° (Figure 1C)). Because lone pairs of N and O atoms were repulsive, conformations of the parent except those mentioned above could not be achieved (Figure S1 in Supporting Information).[30] Similarly, potential energy surfaces of N-substituted compounds at X$_2$ or X$_5$ suggested its stable conformation overlapped with that of the parent (around ϕ3 on 90°, and ϕ4 on 240°), but they could not take another conformation because of N to O (carbonyl) repulsion (around ϕ3 on 90°, and ϕ4 on 60°; Figure 1B and Supporting Information Figure S5). The same tendency was observed at X$_1$ of ϕ1−ϕ2 (see Supporting Information for calculated data of
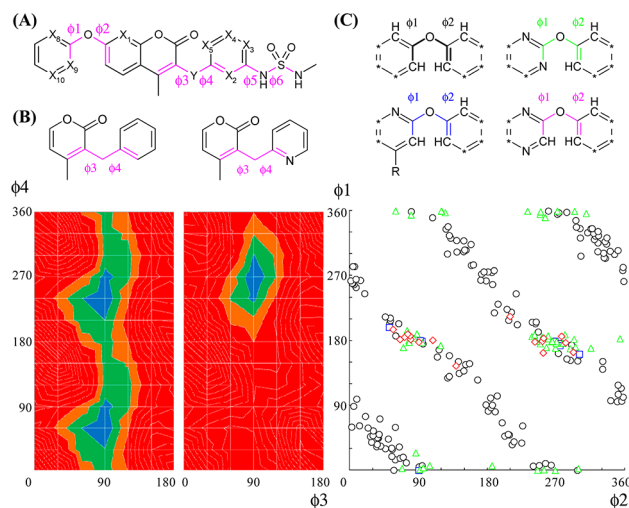

Figure 1. (A) Rotatable bonds of our compound. (B) Potential energy surfaces calculated at the B3LYP/6-31(d) level. The ΔE from 0 to 5 kJ/mol is colored in blue, 5−10 kJ/mol in green, 10−15 kJ/mol in brown, and >15 kJ/mol in red. (C) Torsional distributions in small molecule crystal structures from the CSD data (* = C−R or N).

this and other values below). Structural difference for ϕ3−ϕ4 at X$_3$ or X$_4$ could be minimal. Fixation of sulfamide by intramolecular hydrogen bonding was suggested in ϕ5−ϕ6 at X$_2$ or X$_3$ by potential energy surfaces (Supporting Information Figure S6), while there were smaller effects at X$_4$ or X$_5$. Thus, two positions (X$_{10}$ and X$_4$) could afford smaller effects on the whole 3D structure (most preferred conformations of the parent would be acceptable), and the reason for their reduced bioactivity would be attributed to reason 2. Compounds after nitrogen substitution of six positions (X$_1$, X$_2$, X$_3$, X$_5$, X$_8$, and X$_9$) could inherit some stable conformations of the parent, but not others, because of intramolecular electrostatic repulsion and/or formation of hydrogen bonds. Three of them (X$_3$, X$_8$, and X$_9$) retained bioactivity, and the other three reduced it (though the reason for reduced bioactivity could not be identified). We considered that our nitrogen scanning worked because at least some stable conformations could overlap with the parent in most derivatives after nitrogen substitution.

After further development of compounds **1**[20] and **14**[2] by pharmacology and PK profiles, we selected compound **1** for clinical trial. Compound **1** showed excellent PK data for mouse, rat, and monkey with bioavailability values comparable to compound **14** (compound **1**, 93%, 66%, and 82%, and **14**, 75%, 84%, and 59%, respectively) and better clearance values (compound **1**, 1.1, 0.7, and 0.1 mL/min/kg, and **14**, 6.8, 6.6, and 0.9 mL/min/kg, respectively). A potent antitumor effect of both compounds was observed in the C32 xenograft model (IC$_{50}$s on C32 (B-Raf V600E) cell growth of compound **1**, 47 nM, and **14**, 57 nM): comparable maximum efficacy (TGI of compound **1**, 118%; **14**, 96%) and 16-fold smaller doses in compound **1** (ED$_{50}$ of compound **1**, 0.09 mg/kg, and **14**, 1.44 mg/kg), which reflected the improvement in metabolic stability after nitrogen substitution (Figure 2 and Supporting Information). Neither compound showed serious effects on body weight or any adverse clinical signs.

Salt screening was executed to identify the active pharmaceutical ingredient (API), and crystalline K salts from compound **1** and **14** were found as the candidates.[31] The supersaturated solubility of the K salt of compound **1** in fasted
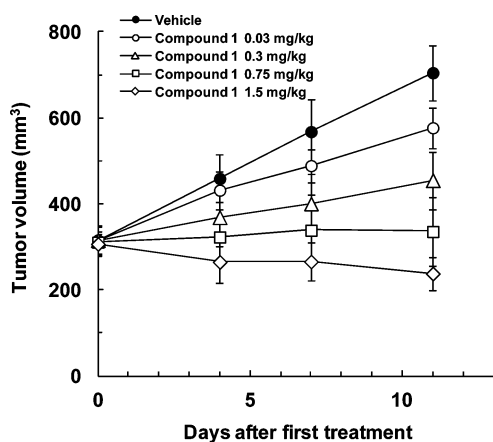
Figure 2. In vivo efficacy of **1** (K salt) in the C32 human malignant melanoma xenograft model. C32 cells were inoculated subcutaneously into the right flank of BALB-nu/nu mice. Tumors were allowed to establish growth after implantation before start of treatment. Coumarin **1** was administered orally once daily for 11 days, from day 0 to day 10. Tumor size was measured twice per week. Values are mean ± SD, $n = 4$.

state simulated intestinal fluid (FaSSIF) after 4 h in a nonsink condition using a mini-scale dissolution test afforded 5-fold greater value (57 μg/mL) than that of compound **14** (12 μg/mL).[32] However, nitrogen substituted compound **1** has comparable saturated solubility to the corresponding **14** regarding crystalline acids (free form). The saturated solubility of compounds **1** and **14** was determined after 24 h equilibration in FaSSIF, which gave 2.7 and 5.5 μg/mL, respectively.[33] It is interesting that nitrogen substitution does not always contribute to increasing the saturated solubility in the free crystalline form; however, it still has an advantage for drug absorption in human because it contributes to increasing the ability to generate and keep the supersaturated state. Judging from these experiments, we selected the salt form of compound **1** (CH5126766/RO5126766)[20] for clinical trial.

In summary, lead optimization of our leads **11a** and **13g** by nitrogen scanning at nine different positions worked effectively to improve the physicochemical properties such as metabolic stability and solubility, as evaluated by high-throughput assay. Changes by nitrogen substitution on the interactions between a derivative and its on- and off-target proteins (Raf/MEK, CYPs, and hERG channel) have an impact, and we focused on identifying the positions for maintaining Raf/MEK activity. Changes in electronic structure created synthetic difficulties because of the difference in reactivity of each nitrogen-containing building block. A candidate with nitrogen introduced could have an advantage in drug absorption, especially if supersaturated formulations, including a salt formation, were developed. We have demonstrated that, in late stage lead optimization, not only the fluorine scan but also the nitrogen scan worked efficiently to select the best compound for clinical use.

■ ASSOCIATED CONTENT

Ⓢ Supporting Information

Experimental preparation of compounds, characterization, biological data, in vitro physicochemical properties, conformational analysis results, and in vivo experimental data. This material is available free of charge via the Internet at http://pubs.acs.org.

■ AUTHOR INFORMATION

Corresponding Author

*(H.I.) Phone: +81-550-87-8597. Fax: +81-550-87-5326. E-mail: iikurahts@chugai-pharm.co.jp.

Author Contributions

The manuscript was written through contributions of all authors.

Notes

The authors declare no competing financial interest.

■ ABBREVIATIONS

AIBN, 2,2′-azodiisobutyronitrile; AUC, area under the curve; BINAP, 2,2′-bis(diphenylphosphino)-1,1′-binaphthyl; CL, clearance; CSD, Cambridge Structural Database; CYP, cytochrome P450; dba, dibenzylideneacetone; DMAP, 4-dimethylaminopyridine; ERK, extracellular signal-regulated kinase; hERG, human ether-a-go-go related gene; HPCD, 2-hydroxypropyl-β-cyclodextrin; LDA, lithium diisopropylamide; LYSA, lyophilized solubility assay; MEK, mitogen-activated protein kinase kinase; NADPH, nicotinamide adenine dinucleotide phosphate (reduced); NBS, N-bromosuccinimide; ND, no data; PAMPA, parallel artificial membrane permeability assay; PEG, polyethylene glycol; PK, pharmacokinetics; TBAF, tetra-n-butylammonium fluoride; TGI, tumor growth inhibition

■ REFERENCES

(1) The effect of fluorine substitution could vary depending on the presence or absence of subsets of neighboring functional groups. See refs 2−5 and references therein.

(2) Hyohdoh, I.; Furuichi, N.; Aoki, T.; Itezono, Y.; Shirai, H.; Ozawa, S.; Watanabe, F.; Matsushita, M.; Sakaitani, M.; Ho, P.-S.; Takanashi, K.; Harada, N.; Tomii, Y.; Yoshinari, K.; Ori, K.; Tabo, M.; Aoki, Y.; Shimma, N.; Iikura, H. Fluorine scanning by non-selective fluorination: enhancing Raf/MEK inhibition while keeping physicochemical properties. *ACS Med. Chem. Lett.* **2013**, *4*, 1059−1063.

(3) Müller, K.; Faeh, C.; Diederich, F. Fluorine in pharmaceuticals: looking beyond intuition. *Science* **2007**, *317*, 1881−1886.

(4) Hagmann, W. K. The many roles for fluorine in medicinal chemistry. *J. Med. Chem.* **2008**, *51*, 4359−4369.

(5) Purser, S.; Moore, P. R.; Swallow, S.; Gouverneur, V. Fluorine in medicinal chemistry. *Chem. Soc. Rev.* **2008**, *37*, 320−330.

(6) Wang, T.; Yin, Z.; Zhang, Z.; Bender, J. A.; Yang, Z.; Johnson, G.; Yang, Z.; Zadjura, L. M.; D'Arienzo, C. J.; DiGiugno Parker, D.; Gesenberg, C.; Yamanaka, G. A.; Gong, Y.-F.; Ho, H.-T.; Fang, H.; Zhou, N.; McAuliffe, B. V.; Eggers, B. J.; Fan, L.; Nowicka-Sans, B.; Dicker, I. B.; Gao, Q.; Colonno, R. J.; Lin, P.-F.; Meanwell, N. A.; Kadow, J. F. Inhibitors of human immunodeficiency virus type 1 (HIV-1) attachment. 5. An evolution from indole to azaindoles leading to the discovery of 1-(4-benzoylpiperazin-1-yl)-2-(4,7-dimethoxy-1H-pyrrolo[2,3-c]pyridin-3-yl)ethane-1,2-dione (BMS-488043), a drug candidate that demonstrates antiviral activity in HIV-1-infected subjects. *J. Med. Chem.* **2009**, *52*, 7778−7787.

(7) Tung, Y.-S.; Coumar, M. S.; Wu, Y.-S.; Shiao, H.-Y.; Chang, J.-Y.; Liou, J.-P.; Shukla, P.; Chang, C.-W.; Chang, C.-Y.; Kuo, C.-C.; Yeh, T.-K.; Lin, C.-Y.; Wu, J.-S.; Wu, S.-Y.; Liao, C.-C.; Hsieh, H.-P. Scaffold-hopping strategy: synthesis and biological evaluation of 5,6-fused bicyclic heteroaromatics to identify orally bioavailable anticancer agents. *J. Med. Chem.* **2011**, *54*, 3076−3080.

313

dx.doi.org/10.1021/ml400379x | *ACS Med. Chem. Lett.* 2014, 5, 309−314

(8) Pennington, L. D.; Croghan, M. D.; Sham, K. K. C.; Pickrell, A. J.; Harrington, P. E.; Frohn, M. J.; Lanman, B. A.; Reed, A. B.; Lee, M. R.; Xu, H.; McElvain, M.; Xu, Y.; Zhang, X.; Fiorino, M.; Horner, M.; Morrison, H. G.; Arnett, H. A.; Fotsch, C.; Tasker, A. S.; Wong, M.; Cee, V. J. Quinolinone-based agonists of S1P₁: Use of a N-scan SAR strategy to optimize in vitro and in vivo activity. *Bioorg. Med. Chem. Lett.* **2012**, *22*, 527−531.

(9) Duplantier, A. J.; Becker, S. L.; Bohanon, M. J.; Borzilleri, K. A.; Chrunyk, B. A.; Downs, J. T.; Hu, L.-Y.; El-Kattan, A.; James, L. C.; Liu, S.; Lu, J.; Maklad, N.; Mansour, M. N.; Mente, S.; Piotrowski, M. A.; Sakya, S. M.; Sheehan, S.; Steyn, S. J.; Strick, C. A.; Williams, V. A.; Zhang, L. Discovery, SAR, and pharmacokinetics of a novel 3-hydroxyquinolin-2(1*H*)-one series of potent D-amino acid oxidase (DAAO) inhibitors. *J. Med. Chem.* **2009**, *52*, 3576−3585.

(10) Jamieson, C.; Moir, E. M.; Rankovic, Z.; Wishart, G. Medicinal chemistry of hERG optimizations: highlights and hang-ups. *J. Med. Chem.* **2006**, *49*, 5029−5046.

(11) Aronov, A. M. Ligand structural aspects of hERG channel blockade. *Curr. Top. Med. Chem.* **2008**, *8*, 1113−1127.

(12) Meanwell, N. A. Improving drug candidates by design: a focus on physicochemical properties as a means of improving compound disposition and safety. *Chem. Res. Toxicol.* **2011**, *24*, 1420−1456.

(13) Rowley, M.; Hallett, D. J.; Goodacre, S.; Moyes, C.; Crawforth, J.; Sparey, T. J.; Patel, S.; Marwood, R.; Patel, S.; Thomas, S.; Hitzel, L.; O'Connor, D.; Szeto, N.; Castro, J. L.; Hutson, P. H.; MacLeod, A. M. 3-(4-Fluoropiperidin-3-yl)-2-phenylindoles as high affinity, selective, and orally bioavailable h5-HT₂ₐ receptor antagonists. *J. Med. Chem.* **2001**, *44*, 1603−1614.

(14) Shen, H. C.; Ding, F.-X.; Wang, S.; Deng, Q.; Zhang, X.; Chen, Y.; Zhou, G.; Xu, S.; Chen, H.-S.; Tong, X.; Tong, V.; Mitra, K.; Kumar, S.; Tsai, C.; Stevenson, A. S.; Pai, L.-Y.; Alonso-Galicia, M.; Chen, X.; Soisson, S. M.; Roy, S.; Zhang, B.; Tata, J. R.; Berger, J. P.; Colletti, S. L. Discovery of a highly potent, selective, and bioavailable soluble epoxide hydrolase inhibitor with excellent ex vivo target engagement. *J. Med. Chem.* **2009**, *52*, 5009−5012.

(15) Du, L.; Li, M.; You, Q. The interactions between *h*ERG potassium channel and blockers. *Curr. Top. Med. Chem.* **2009**, *9*, 330−338.

(16) Ahlström, M. M.; Zamora, I. Characterization of type II ligands in CYP2C9 and CYP3A4. *J. Med. Chem.* **2008**, *51*, 1755−1763.

(17) Leach, A. G.; Kidley, N. J. Quantitatively interpreted enhanced inhibition of cytochrome P450s by heteroaromatic rings containing nitrogen. *J. Chem. Inf. Model* **2011**, *51*, 1048−1063.

(18) Aoki, T.; Hyohdoh, I.; Furuichi, N.; Ozawa, S.; Watanabe, F.; Matsushita, M.; Sakaitani, M.; Ori, K.; Takanashi, K.; Harada, N.; Tomii, Y.; Tabo, M.; Yoshinari, K.; Aoki, Y.; Shimma, N.; Iikura, H. The sulfamide moiety affords higher inhibitory activity and oral bioavailability to a series of coumarin dual selective RAF/MEK inhibitors. *Bioorg. Med. Chem. Lett.* **2013**, *23*, 6223−6227.

(19) Friday, B. B.; Adjei, A. A. K-ras as a target for cancer therapy. *Biochim. Biophys. Acta* **2005**, *1756*, 127−144.

(20) Ishii, N.; Harada, N.; Joseph, E. W.; Ohara, K.; Miura, T.; Sakamoto, H.; Matsuda, Y.; Tomii, Y.; Tachibana-Kondo, Y.; Iikura, H.; Aoki, T.; Shimma, N.; Arisawa, M.; Sowa, Y.; Poulikakos, P. I.; Rosen, N.; Aoki, Y.; Sakai, T. Enhanced inhibition of ERK signaling by a novel allosteric MEK inhibitor, CH5126766, that suppresses feedback reactivation of RAF activity. *Cancer Res.* **2013**, *73*, 4050−4060.

(21) Cheng, J.-F.; Chen, M.; Wallace, D.; Tith, S.; Arrhenius, T.; Kashiwagi, H.; Ono, Y.; Ishikawa, A.; Sato, H.; Kozono, T.; Sato, H.; Nadzan, A. M. Discovery and structure−activity relationship of coumarin derivatives as TNF-*α* inhibitors. *Bioorg. Med. Chem. Lett.* **2004**, *14*, 2411−2415.

(22) Schultz, A. G.; Hagmann, W. K. Synthesis of indole-2-carboxylic esters. *J. Org. Chem.* **1978**, *43*, 3391−3393.

(23) Atkins, R. L.; Bliss, D. E. Substituted coumarins and azacoumarins. Synthesis and fluorescent properties. *J. Org. Chem.* **1978**, *43*, 1975−1980.

(24) Majumdar, K. C.; Debnath, P.; Roy, B. Metal-catalyzed heterocyclization: formation of five- and six-membered oxygen heterocycles through carbon-oxygen bond forming reactions. *Heterocycles* **2009**, *78*, 2661−2728.

(25) Alsenz, J.; Kansy, M. High throughput solubility measurement in drug discovery and development. *Adv. Drug Delivery Rev.* **2007**, *59*, 546−567.

(26) Kansy, M.; Senner, F.; Gubernator, K. Physicochemical high throughput screening: parallel artificial membrane permeation assay in the description of passive absorption processes. *J. Med. Chem.* **1998**, *41*, 1007−1010.

(27) Some reports suggested that lipophilic compounds or aromatic moieties tend to inhibit CYP more strongly. See refs 12, 28, and 29.

(28) Gleeson, M. P.; Davis, A. M.; Chohan, K. K.; Paine, S. W.; Boyer, S.; Gavaghan, C. L.; Arnby, C. H.; Kankkonen, C.; Albertson, N. Generation of in-silico cytochrome P450 1A2, 2C9, 2C19, 2D6, and 3A4 inhibition QSAR models. *J. Comput.-Aided Mol. Des.* **2007**, *21*, 559−573.

(29) Lewis, D. F. V.; Lake, B. G.; Dickins, M. Quantitative structure−activity relationships (QSARs) in CYP3A4 inhibitors: The importance of lipophilic character and hydrogen bonding. *J. Enzyme Inhib. Med. Chem.* **2006**, *21*, 127−132.

(30) Chein, R.-J.; Corey, E. J. Strong conformational preferences of heteroaromatic ethers and electron pair repulsion. *Org. Lett.* **2010**, *12*, 132−135.

(31) The sulfamide could form a salt easily (see ref 18). The pK_as of compound **1** and **14** were 7.02 and 8.86, respectively.

(32) Takano, R.; Sugano, K.; Higashida, A.; Hayashi, Y.; Machida, M.; Aso, Y.; Yamashita, S. Oral absorption of poorly water-soluble drugs: computer simulation of fraction absorbed in humans from a miniscale dissolution test. *Pharm. Res.* **2006**, *23*, 1144−1156.

(33) Our LYSA method measured the ability to keep a super-saturated state by dissolving concentrated DMSO solution of the compounds in water (see Supporting Information). In our lead optimization, we did not measure saturated solubility from a crystalline acid, which could correlate with the melting point.

■ NOTE ADDED AFTER ASAP PUBLICATION

Due to a production error, this paper published ASAP on January 24, 2014 without its required corrections. The revised version was reposted on January 27, 2014.

314

dx.doi.org/10.1021/ml400379x | *ACS Med. Chem. Lett.* 2014, 5, 309−314